INTERNATIONAL JOURNAL FOR NUMERICAL METHODS IN FLUIDS
Int. J. Numer. Meth. Fluids **28**: 395–418 (1998)

ON RIEMANN SOLVERS FOR COMPRESSIBLE LIQUIDS

M.J. IVINGS*, D.M. CAUSON AND E.F. TORO

Department of Mathematics and Physics, Manchester Metropolitan University, Chester Street, Manchester M1 5GD, UK

SUMMARY

A number of Riemann solvers are proposed for the solution of the Riemann problem in a compressible liquid. Both the Tait and Tammann equations of state are used to describe the liquid. Along with exact Riemann solvers, a detailed description of a primitive variable Riemann solver, a two-shock Riemann solver, a two-rarefaction Riemann solver and an extension to the HLL Riemann solver, namely the HLLC Riemann solver, are presented. It is shown how these Riemann solvers may be implemented into Godunov-type numerical methods. The appropriateness of each of the Riemann solvers for a number of flow situations is demonstrated by applying Godunov's method to some revealing shock tube test problems. © 1998 John Wiley & Sons, Ltd.

KEY WORDS: compressible liquid; Riemann solvers; approximate Riemann solvers; Tammann equation of state; Tait equation of state

1. INTRODUCTION

The study of compressible gas dynamics has been far more extensive than that for compressible hydrodynamics. This paper provides methods for solving the equations of hydrodynamics using some ideas developed in the study of gas dynamics. In the main, the desire to solve the Riemann problem for a liquid is to use the solution as part of a Godunov-type numerical scheme for solving general multidimensional initial boundary value problems for shock wave propagation in liquids. However, the solution to the Riemann problem in a liquid also leads to a better understanding of its properties. As the exact Riemann solution is often too time consuming to use effectively as part of a numerical scheme, a number of approximate Riemann solvers are also presented. These Riemann solvers lead directly, without need for iteration, to an approximate solution for the Riemann problem. The hydrodynamic equations are taken to be the inviscid, compressible Euler equations describing the conservation of mass, momentum and total energy.

To describe a liquid, a suitable equation of state is required; here the Tait [1] and Tammann [2] equations of state, which are applicable to a wide range of liquids, shall be used. The Tait equation appears to be the more widely used of the two (e.g [3,4]), and it is used to describe the homentropic flow of a liquid, i.e. entropy is the same for all fluid particles. In fact, the modified Tait equation of state proposed by Kirkwood [5], which bears little resemblance to the original Tait equation of state, derived from measurements of seawater [6] will be used. The

* Correspondence to: Department of Mathematics and Physics, Manchester Metropolitan University, Chester Street, Manchester M1 5GD, UK.

CCC 0271–2091/98/130395–24$17.50

Received March 1997
Revised June 1997

modified Tait equation of state is an excellent representation of the equation of state for a number of liquids under a wide range of temperatures and pressures [7], e.g. it is suitable as an equation of state for water up to 25000 atmospheres. The Tammann equation of state is suitable for describing liquids at high pressures [2,8] and if the flow is isentropic, the Tammann equation of state appears to be in good agreement with the Tait equation of state [9,10]. However, the Tammann equation of state is more suitable for flows undergoing non-isentropic processes, such as shock waves. A review of other equations of state for water can be found in Reference [10]. Examples of areas where the study of compressible liquids may be of interest include underwater explosions [4], oil flow in shock absorbers [3] and extracorporeal shock wave lithotripsy (ESWL) used for the removal of kidney stones where the acoustic properties of tissue are very similar to those for water. The numerical solution of compressible hydrodynamic problems has not received a large amount of attention. However, an exact Riemann solver employing the Tait equation of state has been used by both Flores and Holt [4] and by Sugimura *et al.* [8]. This Riemann solver will prove satisfactory for one-dimensional problems, but it is not fast enough to be used effectively in more complex multidimensional problems. Finite difference approaches that have been used to solve problems of this kind include that by Cooke and Chen [11], who used Roe's method with both the Tait equation of state and a general equation of state to provide the solution to some one-dimensional test problems. Koren *et al.* [3] uses an Osher type scheme to solve an oil flow problem in which a linearised version of the Tait equation of state is used to describe the oil. The present Riemann solvers provide a firm base upon which numerical schemes can be built, with the aim of solving complex multidimensional initial boundary value problems.

The rest of this paper is set out as follows; Section 2 introduces the governing equations for the fluid dynamics of a compressible liquid and its equation of state. In Section 3, two exact Riemann solvers using the Tammann and Tait equations of state, respectively, are presented. Four approximate Riemann solvers are presented in Section 4. Finally, a number of test problems are presented in Section 5 to assess the performance of the Riemann solvers and some conclusions can be found in Section 6.

2. THE RIEMANN PROBLEM

Here two equations of state for a liquid shall be considered, namely the Tammann and (modified) Tait equations of state. The Tammann equation of state can be written as

$$p = p(\rho, e) = (\gamma - 1)\rho e - \gamma p_c, \tag{1}$$

where p, ρ and e are the pressure, density and specific internal energy, respectively. The values for the pressure constant, p_c, and polytropic constant, γ, are liquid-dependent, and a number of these values corresponding to a number of different liquids can be found in Reference [12]. Note that if $1 < \gamma < 2$ and $p_c = 0$, the Tammann equation of state reduces to the ideal gas equation of state; this is a very useful property of this equation of state. The sound speed associated with this equation of state is given by

$$a^2 = \frac{\gamma}{\rho}(p + p_c). \tag{2}$$

The Tait equation of state can be written as

$$p = p(\rho) = B\left[\left(\frac{\rho}{\rho_0}\right)^n - 1\right], \tag{3}$$

where B is a pressure constant that is in fact a weak function of entropy but is usually treated as a constant. The density of the liquid at atmospheric pressure is denoted by ρ_0, and n is a constant playing a similar role to the ratio of specific heats for an ideal gas. Different values for these constants corresponding to a number of different liquids can be found in Reference [1]. The corresponding sound speed for the Tait equation of state is given by

$$a^2 = \frac{n}{\rho}(p + B). \tag{4}$$

The Riemann problem is the initial value problem for a hyperbolic system of conservations laws,

$$\mathbf{U}_t + \mathbf{F}(\mathbf{U})_x = 0, \tag{5}$$

with initial conditions consisting simply of two constant states separated by a discontinuity

$$\mathbf{U}_0(x) = \begin{cases} \mathbf{U}_\mathrm{L} & x < 0 \\ \mathbf{U}_\mathrm{R} & x > 0. \end{cases} \tag{6}$$

Computationally, interest is in two- and three-dimensional problems. From a numerical point of view, it is sufficient to consider the Riemann problem in the direction normal to the interface of a computing cell. Provisionally assuming Cartesian co-ordinates, it suffices to consider the Riemann problem in the x-direction. Here, the two-dimensional x-split Euler equations are studied, in which case the set of conserved variables, $\mathbf{U}$, and the corresponding fluxes, $\mathbf{F}(\mathbf{U})$, are

$$\mathbf{U} = \begin{pmatrix} \rho \\ \rho u \\ \rho v \\ E \end{pmatrix}, \qquad \mathbf{F}(\mathbf{U}) = \begin{pmatrix} \rho u \\ \rho u^2 + p \\ \rho uv \\ u(E + p) \end{pmatrix}, \tag{7}$$

where u is the particle velocity in the x-direction, v is the tangential particle velocity and E is the total energy per unit volume, $E = \rho(e + \frac{1}{2}(u^2 + v^2))$. However, in the case for the Tait equation of state, the pressure is a function of density, only in which case, the internal energy can be written as $e = e^{(1)}(\rho) + e^{(2)}(S)$ [13], where S is the entropy. This in turn allows the elimination of the energy equation from (7) and thus the (isentropic) Euler equations become

$$\begin{pmatrix} \rho \\ \rho u \\ \rho v \end{pmatrix}_t + \begin{pmatrix} \rho u \\ \rho u^2 + k\rho^n \\ \rho uv \end{pmatrix}_x = 0, \tag{8}$$

where $k = B/\rho_0{}^n$. As one would expect, this simplification influences the solution to the Riemann problem.

The solution to the Riemann problem is a similarity solution in that it is a function of x/t only. The solution to the Riemann problem using the Tammann equation of state (see Figure 1) consists of two non-linear waves which are either shocks or rarefactions. The middle wave in Figure 1 is actually a contact wave and a shear wave travelling at the same speed, this corresponds to the repeated eigenvalue of the Jacobian of $\mathbf{F}(\mathbf{U})$. The solution to the Riemann

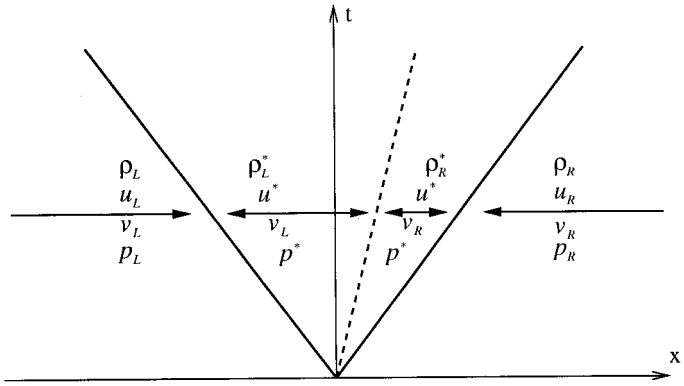

Figure 1. Wave diagram showing the structure of a typical solution to the x-split two-dimensional Riemann problem using the Tammann equation of state.

problem using the Tait equation of state consists of two non-linear waves and a shear wave, see Figure 2. In both cases, the region between the two non-linear waves is called the star region, the pressure p_* and particle velocity u_* are constant in this region. The tangential velocity component, v, is discontinuous across the shear wave and in the Tammann equation of state case, the density varies discontinuously from ρ_{L}^* to ρ_{R}^* across the contact wave. For a general background in Riemann solvers see Reference [14].

3. TWO EXACT RIEMANN SOLVERS

The exact solution to the Riemann problem is obtained by constructing a function $f(q)$, relating the two data states to a q variable in the star region, and then solving the single non-linear algebraic equation $f(q) = 0$. This equation is solved by a Newton–Raphson iteration, the remaining star state variables then follow directly along with the wave speeds. As the solution method for each equation of state differs, the details for each will be presented in turn.

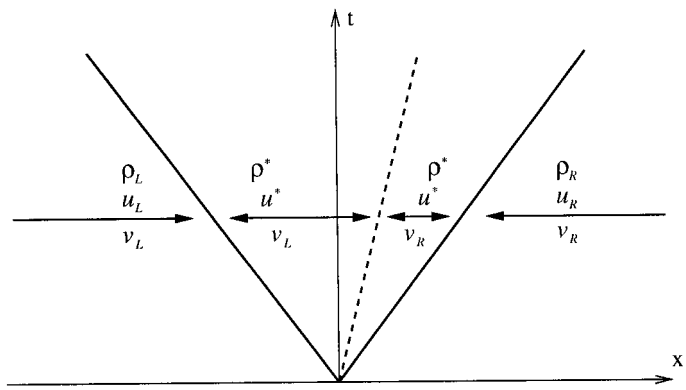

Figure 2. Wave diagram showing the structure of a typical solution to the x-split two-dimensional Riemann problem using the Tait equation of state.

3.1. An exact Riemann solver using the Tammann equation of state

The exact solution to the Riemann problem is obtained by solving a single non-linear algebraic equation for p^*,

$$f(p_*) = 0. \tag{9}$$

To relate p^* to the left and right data states using relationships across the left and right (non-linear) waves, Equation (9) is written as

$$f(p_*) \equiv f_L(\mathbf{U}_L, p_*) + f_R(\mathbf{U}_R, p_*) + \Delta u = 0, \tag{10}$$

where $\Delta u = u_R - u_L$. Since the non-linear waves are either shock waves or rarefaction waves there are two possible formulations for f_K (K = L or R).

3.1.1. Shock wave relations. In order to derive a relationship across the shock wave, the Rankine–Hugoniot conditions are required; these can be written as

$$\rho_K w_K = \rho_K^* w_*, \tag{11}$$

$$\rho_K w_K^2 + p_K = \rho_K^* w_*^2 + p_*, \tag{12}$$

$$\frac{1}{2} w_K^2 + h_K = \frac{1}{2} w_*^2 + h_K^*, \tag{13}$$

where K = L or R, the specific enthalpy $h = e + (p/\rho)$ and w is the particle velocity in a frame of reference moving with the shock,

$$w_K = u_K - S_K, \qquad w_* = u_* - S_K; \tag{14}$$

S_K is the shock speed. Now the mass fluxes are defined

$$Q_L = \rho_L w_L = \rho_K^* w_*, \tag{15}$$

and

$$Q_R = -\rho_R w_R = -\rho_R^* w_*. \tag{16}$$

Substitution into Equation (12) gives

$$Q_L = \frac{p_* - p_L}{w_L - w_*} \equiv \frac{\bar{p}_* - \bar{p}_L}{u_L - u_*}, \tag{17}$$

and

$$Q_R = \frac{p_* - p_R}{w_R - w_*} \equiv -\frac{\bar{p}_* - \bar{p}_R}{u_R - u_*}, \tag{18}$$

where $\bar{p} = p + p_c$, which is rearranged to define f_L and f_R

$$u_* = u_L - f_L, \qquad u_* = u_R + f_R. \tag{19}$$

where the functions f_L, f_R are

$$f_L = \frac{\bar{p}_* - \bar{p}_L}{Q_L}, \qquad f_R = \frac{\bar{p}_* - \bar{p}_R}{Q_R}. \tag{20}$$

Eliminating w from Equations (15)–(18),one can solve for Q_K to give

$$Q_{\mathrm{K}} = \left[\rho_{\mathrm{K}} \rho_{\mathrm{K}}^{*} \left(\frac{\bar{p}_{*} - \bar{p}_{\mathrm{K}}}{\rho_{\mathrm{K}}^{*} - \rho_{\mathrm{K}}} \right) \right]^{1/2}. \tag{21}$$

The Tammann equation of state in terms of the specific enthalpy, h, can be written as

$$h = \left(\frac{\gamma}{\gamma - 1} \right) \frac{p + p_{\mathrm{c}}}{\rho}. \tag{22}$$

Eliminating w_{K} and w_{*} from Equation (13) using Equations (11) and (12), the following is obtained

$$h_{\mathrm{K}}^{*} - h_{\mathrm{K}} = \frac{1}{2} \left(\frac{1}{\rho_{\mathrm{K}}} + \frac{1}{\rho_{\mathrm{K}}^{*}} \right) (\bar{p}_{*} - \bar{p}_{\mathrm{K}}), \tag{23}$$

then substituting (22) into (23) gives the density–pressure relation

$$\rho_{\mathrm{K}}^{*} = \rho_{\mathrm{K}} \left[\frac{\dfrac{\bar{p}_{*}}{\bar{p}_{\mathrm{K}}} + \left(\dfrac{\gamma - 1}{\gamma + 1} \right)}{\dfrac{\bar{p}_{*}}{\bar{p}_{\mathrm{K}}} \left(\dfrac{\gamma - 1}{\gamma + 1} \right) + 1} \right]. \tag{24}$$

Replacing ρ_{K}^{*} from (21) with (24) gives, after some manipulation,

$$Q_{\mathrm{K}} = \left[\frac{\bar{p}_{*} + \beta_{\mathrm{K}}}{\alpha_{\mathrm{K}}} \right]^{1/2}, \tag{25}$$

where

$$\alpha_{\mathrm{K}} = \frac{2}{(\gamma + 1)\rho_{\mathrm{K}}} \quad \text{and} \quad \beta_{\mathrm{K}} = \bar{p}_{\mathrm{K}} \left(\frac{\gamma - 1}{\gamma + 1} \right), \tag{26}$$

and thus,

$$f_{\mathrm{K}} = (p_{*} - p_{\mathrm{K}}) \left[\frac{\alpha_{\mathrm{K}}}{\bar{p}_{*} + \beta_{\mathrm{K}}} \right]^{1/2}. \tag{27}$$

3.1.2. Expansion wave relations. To construct the function across a non-linear wave, when the wave is an expansion wave, the isentropic relationship across it and the constancy of the Riemann invariants are used. The isentropic relationship is

$$\rho_{\mathrm{K}}^{*} = \rho_{\mathrm{K}} \left(\frac{\bar{p}_{*}}{\bar{p}_{\mathrm{K}}} \right)^{1/\gamma}, \tag{28}$$

and the Riemann invariants across the left and right waves, respectively, are

$$u_{\mathrm{L}} + \frac{2a_{\mathrm{L}}}{\gamma - 1} = u_{*} + \frac{2a_{\mathrm{L}}^{*}}{\gamma - 1}, \tag{29}$$

and

$$u_{\mathrm{R}} - \frac{2a_{\mathrm{L}}}{\gamma - 1} = u_{*} - \frac{2a_{\mathrm{R}}^{*}}{\gamma - 1}. \tag{30}$$

Equations (29) and (30) are rewritten, and f_{L} and f_{R} are defined by

$$u_{*} = u_{\mathrm{L}} = f_{\mathrm{L}}, \qquad u_{*} = u_{\mathrm{R}} + f_{\mathrm{R}}, \tag{31}$$

where the functions f_{L} and f_{R} are

$$f_{\mathrm{L}} = \frac{2}{\gamma - 1}(a_{\mathrm{L}}^{*} - a_{\mathrm{L}}), \qquad f_{\mathrm{R}} = \frac{2}{\gamma - 1}(a_{\mathrm{R}}^{*} - a_{\mathrm{R}}). \tag{32}$$

a_{K}^{*} can be replaced by substituting the isentropic relationship into the definition for sound speed, giving

$$f_{\mathrm{K}} = \frac{2a_{\mathrm{K}}}{\gamma - 1}\left(\left(\frac{\bar{p}_{*}}{\bar{p}_{\mathrm{K}}}\right)^{(\gamma - 1)/2\gamma} - 1\right). \tag{33}$$

3.1.2.1. Completing the solution. Now that Equation (10) has been completely defined, it may be solved using a Newton–Raphson iteration

$$p^{(i+1)} = p^{(i)} - \frac{f(p^{(i)})}{f'(p^{(i)})}. \tag{34}$$

It is assumed the solution has converged when the condition

$$\frac{|p^{(i+1)} - p^{(i)}|}{\frac{1}{2}(p^{(i+1)} + p^{(i)})} < \epsilon \tag{35}$$

has been satisfied, typically $\epsilon \approx 10^{-6}$. The initial start up value for the iteration $p^{(i=1)}$ is found using one of the approximate Riemann solvers of Section 4. The star state particle velocity is computed by taking a mean value of the appropriate functions from Equations (19) and (31) to give

$$u_{*} = \frac{1}{2}(u_{\mathrm{L}} + u_{\mathrm{R}}) + \frac{1}{2}(f_{\mathrm{R}}(\bar{p}_{*}) - f_{\mathrm{L}}(\bar{p}_{*})). \tag{36}$$

The densities ρ_{K}^{*} are given by (24) and (28) behind a shock wave and rarefaction wave, respectively. The solution inside a left rarefaction wave along the ray $x/t = u - a$ is given by

$$u = \frac{2}{\gamma + 1}\left(a_{\mathrm{L}} + \frac{1}{2}u_{\mathrm{L}}(\gamma - 1) + \frac{x}{t}\right), \tag{37}$$

$$p = \bar{p}_{\mathrm{L}}\left(\frac{a}{a_{\mathrm{L}}}\right)^{2\gamma/(\gamma - 1)} - p_{\mathrm{c}}, \tag{38}$$

$$\rho = \rho_{\mathrm{L}}\left(\frac{a}{a_{\mathrm{L}}}\right)^{2/(\gamma - 1)}, \tag{39}$$

and along the ray $x/t = u + a$ inside a right rarefaction wave, the solution is

$$u = \frac{2}{\gamma + 1}\left(-a_{\mathrm{R}} + \frac{1}{2}u_{\mathrm{R}}(\gamma - 1) + \frac{x}{t}\right), \tag{40}$$

$$p = \bar{p}_{\mathrm{R}}\left(\frac{a}{a_{\mathrm{R}}}\right)^{2\gamma/(\gamma - 1)} - p_{\mathrm{c}}, \tag{41}$$

$$\rho = \bar{\rho}_{\mathrm{R}}\left(\frac{a}{a_{\mathrm{R}}}\right)^{2/(\gamma - 1)}. \tag{42}$$

All that remains is to calculate the wave speeds. The contact wave obviously travels at speed u_{*}, apart from this expressions are required for the shock speeds and the speeds of the head and tail of a rarefaction wave. The left and right travelling shocks speeds are

$$S_{\mathrm{L}} = u_{\mathrm{L}} - \frac{Q_{\mathrm{L}}}{\rho_{\mathrm{L}}} \quad \text{and} \quad S_{\mathrm{R}} = u_{\mathrm{R}} + \frac{Q_{\mathrm{R}}}{\rho_{\mathrm{R}}}, \tag{43}$$

respectively, where Q_K is given by Equation (25). For a rarefaction wave, the speeds of the head of the wave are

$$\frac{dx}{dt} = u_L - a_L, \qquad \frac{dx}{dt} = u_R + a_R, \tag{44}$$

for a left and right travelling wave, respectively, and the tail of the waves travel with speed

$$\frac{dx}{dt} = u_* - a_L^*, \qquad \frac{dx}{dt} = u_* + a_R^*. \tag{45}$$

3.2. An exact Riemann solver using the Tait equation of state

The exact solution to the Riemann problem using the Tait equation of state is obtained by solving a single non-linear algebraic equation for the density in the star region. The remaining star state variables then follow directly along with the two wave speeds. The function relating the left and right data states to ρ^* can be written as

$$g(\rho_*) \equiv g_L(\mathbf{U}_L, \rho_*) + g_R(\mathbf{U}_R, \rho_*) + \Delta u = 0, \tag{46}$$

where $\Delta u = u_R - u_L$. As in the case for the Tammann equation of state, the left and right functions, g_L and g_R, respectively, depend on whether the non-linear wave is a shock wave or a rarefaction wave.

3.2.1. Shock wave relations. If the non-linear wave is a shock wave, the Rankine–Hugoniot conditions that hold across it are required; these can be written as

$$\rho_K w_K = \rho_* w_*, \tag{47}$$

$$\rho_K w_K^2 + k\rho_K^n = \rho_* w_*^2 + k\rho_*^n, \tag{48}$$

where again, w is the particle velocity in a frame of reference moving with the shock of speed S_K,

$$w_K = u_K - S_K, \qquad w_* = u_* - S_K. \tag{49}$$

Now

$$Q_L = \rho_L w_L = \rho_L^* w_*, \tag{50}$$

and

$$Q_R = -\rho_R w_R = -\rho_R^* w_*. \tag{51}$$

Substituting these into (48) gives

$$Q_L = \frac{k(\rho_*^n - \rho_L^n)}{w_L - w_*} \equiv \frac{k(\rho_*^n - \rho_L^n)}{u_L - u_*}, \tag{52}$$

$$Q_R = \frac{k(\rho_*^n - \rho_R^n)}{w_R - w_*} \equiv \frac{k(\rho_*^n - \rho_R^n)}{u_R - u_*}. \tag{53}$$

These are rearranged to define g_L and g_R

$$u_* = u_L - g_L, \qquad u_* = u_R + g_R, \tag{54}$$

where the left and right functions, g_L and g_R are given by

$$g_{\mathrm{L}} = \frac{k(\rho_*^n - \rho_{\mathrm{L}}^n)}{Q_{\mathrm{L}}} \quad \text{and} \quad g_{\mathrm{R}} = \frac{k(\rho_*^n - \rho_{\mathrm{R}}^n)}{Q_{\mathrm{R}}}. \tag{55}$$

Eliminating w from Equations (50)–(53) gives

$$Q_{\mathrm{K}} = \left[\frac{k(\rho_*^n - \rho_{\mathrm{K}}^n)\rho_{\mathrm{K}}\rho_*}{(\rho_* - \rho_{\mathrm{K}})}\right]^{1/2}, \tag{56}$$

and the result below is obtained

$$g_{\mathrm{K}} = \left[\frac{k(\rho_*^n - \rho_{\mathrm{K}}^n)(\rho_* - \rho_{\mathrm{K}})}{\rho_{\mathrm{K}}\rho_*}\right]^{1/2}. \tag{57}$$

3.2.2. Expansion wave relations. The Riemann invariants across a left and right expansion wave are given by

$$u_* + \frac{2a_*}{(n-1)} = u_{\mathrm{L}} + \frac{2a_{\mathrm{L}}}{(n-1)}, \tag{58}$$

and

$$u_* - \frac{2a_*}{(n-1)} = u_{\mathrm{R}} - \frac{2a_{\mathrm{R}}}{(n-1)}, \tag{59}$$

respectively. A rearrangement of these leads to the definition for g_{K}

$$u_* = u_{\mathrm{L}} - g_{\mathrm{L}}, \qquad u_* = u_{\mathrm{R}} + g_{\mathrm{R}}, \tag{60}$$

where the functions g_{L} and g_{R} are

$$g_{\mathrm{L}} = \frac{2}{n-1}(a_* - a_{\mathrm{L}}), \qquad g_{\mathrm{R}} = \frac{2}{n-1}(a_* - a_{\mathrm{R}}). \tag{61}$$

The sound speed behind the rarefaction wave, a_*, can then be found by substituting the Tait equation into the definition of sound speed to give

$$g_{\mathrm{K}} = \frac{2a_{\mathrm{K}}}{(n-1)}\left[\left(\frac{\rho_*}{\rho_{\mathrm{K}}}\right)^{(n-1)/2} - 1\right]. \tag{62}$$

3.2.2.1. Completing the solution. Equation (46) has now been fully defined and this is solved using a Newton–Raphson iteration,

$$\rho^{(i+1)} = \rho^{(i)} - \frac{g(\rho^{(i)})}{g'(\rho^{(i)})}, \tag{63}$$

where it is assumed the solution has converged when the condition

$$\frac{|\rho^{(i+1)} - \rho^{(i)}|}{\frac{1}{2}(\rho^{(i+1)} + \rho^{(i)})} < \epsilon \tag{64}$$

has been satisfied, typically $\epsilon \approx 10^{-6}$. For a start up value $\rho^{(\mathrm{i}=1)}$, one of the approximate Riemann solvers of Section 4 is used. The star state velocity then follows by taking an average of the two equations for u_* in (54) and (60) as appropriate,

$$u_* = \frac{1}{2}(u_{\mathrm{L}} + u_{\mathrm{R}}) + \frac{1}{2}(g_{\mathrm{R}}(\rho_*) - g_{\mathrm{L}}(\rho_*)). \tag{65}$$

The solution inside a left rarefaction wave along the ray $x/t = u - a$ is given by

$$u = \frac{2}{n+1}\left(a_{\mathrm{L}} + \frac{1}{2}u_{\mathrm{L}}(n-1) + \frac{x}{t}\right), \tag{66}$$

$$\rho = \left(\frac{a^2}{nk}\right)^{1/(n-1)}, \tag{67}$$

and along the ray $x/t = u + a$ inside a right rarefaction wave, the solution is

$$u = \frac{2}{n+1}\left(-a_{\mathrm{R}} + \frac{1}{2}u_{\mathrm{R}}(n-1) + \frac{x}{t}\right), \tag{68}$$

$$\rho = \left(\frac{a^2}{nk}\right)^{1/(n-1)}. \tag{69}$$

The wave speeds are calculated as follows: for a left and right travelling shock wave, respectively, you have

$$S_{\mathrm{L}} = u_{\mathrm{L}} - \frac{Q_{\mathrm{L}}}{\rho_{\mathrm{L}}} \quad \text{and} \quad S_{\mathrm{R}} = u_{\mathrm{R}} + \frac{Q_{\mathrm{R}}}{\rho_{\mathrm{R}}}, \tag{70}$$

where Q_{K} are given by Equation (56). For a rarefaction wave, the speeds of the head of the wave are

$$\frac{\mathrm{d}x}{\mathrm{d}t} = u_{\mathrm{L}} - a_{\mathrm{L}}, \qquad \frac{\mathrm{d}x}{\mathrm{d}t} = u_{\mathrm{R}} + a_{\mathrm{R}}, \tag{71}$$

and the speeds of the tail of the rarefaction wave are

$$\frac{\mathrm{d}x}{\mathrm{d}t} = u^* - a^*_{\mathrm{L}}, \qquad \frac{\mathrm{d}x}{\mathrm{d}t} = u^* + a^*_{\mathrm{R}}. \tag{72}$$

The shear wave travels with speed u^*.

4. APPROXIMATE RIEMANN SOLVERS

The use of a Riemann problem-based numerical scheme to compute the solution to a single initial boundary value problem can require the solution to the Riemann problem many hundreds of thousands of times. It is therefore necessary to provide the solution with a minimum of calculations, and hence CPU time, without unacceptable loss of accuracy. For this reason this paper presents a number of approximate Riemann solvers that lead directly to the solution of the Riemann problem in a liquid. As in the case for the exact Riemann solvers, some methods will be used that were developed in the study of gas dynamics.

4.1. A linearised Riemann solver

This Riemann solver, often known as the primitive variable Riemann solver (PVRS), has been shown to be very accurate for flows in which the shocks are of no more than moderate strength [15]. In the same paper, it is shown that when this Riemann solver is used in an adaptive fashion, with an exact Riemann solver, severe flow problems can be solved quickly with almost indistinguishable accuracy from those where the exact Riemann solver is used exclusively. In short, this Riemann solver exactly solves a linearised version of the primitive variable Euler equations.

4.1.1. The PVRS using the Tammann equation of state. The Euler equations (5) written in primitive variable form, linearised about some average state $\bar{\mathbf{W}} = (\bar{\rho}, \bar{u}, \bar{v}, \bar{p})^T$ are

$$\begin{pmatrix} \rho \\ u \\ v \\ p \end{pmatrix}_t + \begin{bmatrix} \bar{u} & \bar{\rho} & 0 & 0 \\ 0 & \bar{u} & 0 & 1/\bar{\rho} \\ 0 & 0 & \bar{u} & 0 \\ 0 & \bar{\rho}\bar{a}^2 & 0 & \bar{u} \end{bmatrix} \begin{pmatrix} \rho \\ u \\ v \\ p \end{pmatrix}_x = 0. \tag{73}$$

The Riemann problem for this linear system of equations can be solved exactly using standard techniques for linear hyperbolic systems with constant coefficients. The eigenvalues of the matrix in (73)

$$\lambda_1 = \bar{u} - \bar{a}, \qquad \lambda_{2,3} = \bar{u}, \qquad \lambda_4 = \bar{u} + \bar{a}, \tag{74}$$

are associated with the right eigenvectors

$$\bar{R}_1 = \begin{pmatrix} \bar{\rho} \\ -\bar{a} \\ 0 \\ \bar{\rho}\bar{a}^2 \end{pmatrix}, \qquad \bar{R}_2 = \begin{pmatrix} \bar{\rho} \\ 0 \\ 0 \\ 0 \end{pmatrix}, \qquad \bar{R}_3 = \begin{pmatrix} 0 \\ 0 \\ \bar{\rho} \\ 0 \end{pmatrix}, \qquad \bar{R}_4 = \begin{pmatrix} \bar{\rho} \\ \bar{a} \\ 0 \\ \bar{\rho}\bar{a}^2 \end{pmatrix}. \tag{75}$$

The jumps in ρ, u, v, p across the wave structure can be written as

$$\Delta\mathbf{W} = \mathbf{W}_\mathrm{R} - \mathbf{W}_\mathrm{L} = \sum_{i=1}^{4} \eta_i \bar{R}_i. \tag{76}$$

After solving for η_i, the solution to this Riemann problem can be found to be

$$p_* = \frac{1}{2}(p_\mathrm{L} + p_\mathrm{R}) - \frac{1}{2}(u_\mathrm{R} - u_\mathrm{L})\bar{\rho}\bar{a}, \tag{77}$$

$$u_* = \frac{1}{2}(u_\mathrm{L} + u_\mathrm{R}) - \frac{1}{2}\frac{(p_\mathrm{R} - p_\mathrm{L})}{\bar{\rho}\bar{a}} \tag{78}$$

$$\rho_\mathrm{L}^* = \rho_\mathrm{L} + (u_\mathrm{L} - u_*)\frac{\bar{\rho}}{\bar{a}}, \tag{79}$$

$$\rho_\mathrm{R}^* = \rho_\mathrm{R} + (u_* - u_\mathrm{R})\frac{\bar{\rho}}{\bar{a}}. \tag{80}$$

The tangential velocity component v changes discontinuously across the shear wave,

$$v = \begin{cases} v_\mathrm{L} & \text{if} \quad x/t < u^* \\ v_\mathrm{R} & \text{if} \quad x/t > u^* \end{cases}. \tag{81}$$

Note that even though the solution for the tangential velocity component is trivial, some Riemann solvers do actually get this part of the solution wrong. As to the choice for $\bar{\mathbf{W}}$, experience in both gas dynamics and for compressible liquids has shown that the size of the errors introduced by using different estimates for the average states $(\bar{\rho}, \bar{a})$ depend on the initial conditions and specifically, the errors grow as the initial pressure ratio increases. Where this pressure ratio is < 10, different choices for the average states do not significantly affect the

accuracy of the Riemann solver. However, this Riemann solver is particularly suited to adaptive schemes, in which case it is used where the initial pressure ratio is < 2. Therefore, it is believed that the choice of the average states is not critical. Other more sophisticated choices have been derived, e.g. to recognise isolated discontinuities, but their complexity outweighs the benefits and therefore, their use is not recommended, it is suggested that it is sufficient to choose

$$\bar{\rho} = \frac{1}{2}(\rho_L + \rho_R), \qquad \bar{a} = \frac{1}{2}(a_L + a_R). \tag{82}$$

4.1.2. The PVRS using the Tait equation of state. The isentropic Euler equations (8) written in primitive variable form, linearised about some state $\bar{\mathbf{W}} = (\bar{\rho}, \bar{u}, \bar{v})^T$ can be written as

$$\begin{pmatrix} \rho \\ u \\ v \end{pmatrix}_t + \begin{bmatrix} \bar{u} & \bar{\rho} & 0 \\ \bar{a}^2/\bar{\rho} & \bar{u} & 0 \\ 0 & 0 & \bar{u} \end{bmatrix} \begin{pmatrix} \rho \\ u \\ v \end{pmatrix}_x = 0. \tag{83}$$

Here the matrix in (83) has the eigenvalues

$$\lambda_1 = \bar{u} - \bar{a}, \qquad \lambda_2 = \bar{u}, \qquad \lambda_3 = \bar{u} + \bar{a}, \tag{84}$$

with associated eigenvectors

$$\bar{R}_1 = \begin{pmatrix} \bar{\rho} \\ -\bar{a} \\ 0 \end{pmatrix}, \qquad \bar{R}_2 = \begin{pmatrix} 0 \\ 0 \\ \bar{\rho} \end{pmatrix}, \qquad \bar{R}_3 = \begin{pmatrix} \bar{\rho} \\ \bar{a} \\ 0 \end{pmatrix}. \tag{85}$$

The exact solution to the Riemann problem governed by this set of linear equations can be found by writing the jumps in ρ, u and v across each wave as the sum

$$\Delta\mathbf{W} = \mathbf{W}_R - \mathbf{W}_L = \sum_{i=1}^{3} \eta_i \bar{R}_i, \tag{86}$$

and solving, first for η_i, and then ρ_* and u_*, to obtain

$$\rho_* = \frac{1}{2}(\rho_L + \rho_R) - \frac{1}{2}(u_R - u_L)\frac{\bar{\rho}}{\bar{a}}, \tag{87}$$

$$u_* = \frac{1}{2}(u_L + u_R) - \frac{1}{2}(\rho_R - \rho_L)\frac{\bar{a}}{\bar{\rho}}, \tag{88}$$

where $\bar{\rho}$ and $\bar{a}$ are again calculated from Equation (82), and the tangential velocity component is given by Equation (81).

4.2. A two-rarefaction Riemann solver

If the assumption that the solution of the Riemann problem contains two rarefaction waves is made, the solution can be directly computed. For details on the two-rarefaction Riemann solver (TRRS) for gas dynamics see Reference [16].

4.2.1. The TRRS using the Tammann equation of state. If the two equations for u^* given by (31) are equated, you get the closed form approximation for p^*,

$$p^* = \left[\frac{a_L + a_R - \frac{1}{2}(\gamma - 1)\Delta u}{\frac{a_L}{\bar{p}_L^z} + \frac{a_R}{\bar{p}_R^z}} \right]^{1/z} - p_c, \tag{89}$$

where $z = (\gamma - 1)/2\gamma$. The particle velocity then follows as

$$u^* = \frac{\frac{\bar{p}^*}{\bar{p}_L}\frac{u_L}{a_L} + \frac{u_R}{a_R} + 2\left(\frac{\bar{p}^*}{\bar{p}_L} - 1\right)/(\gamma - 1)}{\frac{\bar{p}^*}{\bar{p}_L}\frac{1}{a_L} + \frac{1}{a_R}}. \tag{90}$$

The density star states ρ_L^* and ρ_R^* then simply follow from the isentropic relationships (28) and the tangential velocity is given by Equation (81).

4.2.2. The TRRS using the Tait equation of state. This Riemann solver provides a very simple solution when used with the Tait equation of state. The equations for the left and right Riemann invariants (58) and (59) can be solved for u^* and a^*

$$u_* = \frac{1}{2}(u_L + u_R) - \frac{1}{n-1}(a_R - a_L), \tag{91}$$

$$a_* = \frac{1}{2}(a_L + a_R) - \frac{1}{4}(n-1)(u_R - u_L). \tag{92}$$

Use of the Tait equation of state and the definition for sound speed gives

$$\rho_* = \left(\frac{a_*^2}{nk}\right)^{1/(n-1)}. \tag{93}$$

The solution is completed by computing the tangential velocity from (81).

4.3. A two-shock Riemann solver

This two-shock Riemann solver (TSRS), originally proposed for gas dynamics [16], makes the assumption that the solution to the Riemann problem contains two shock waves. Unfortunately, the solution does not immediately come out directly as in the case for the TRRS. It is shown below how this is overcome, to produce a very accurate approximate Riemann solver.

4.3.1. The TSRS using the Tammann equation of state. If the two equations for the particle velocity u^* behind a shock wave are equated, although a solution for p^* cannot be found directly, it can written

$$p_* = \frac{p_L \bar{f}_L(p^{(0)}) + p_R \bar{f}_R(p^{(0)}) - \Delta u}{\bar{f}_L(p^{(0)}) + \bar{f}_R(p^{(0)})}, \tag{94}$$

where

$$\bar{f}_K = \left[\frac{\alpha_K}{p^{(0)} + p_c + \beta_K}\right]^{1/2}, \tag{95}$$

and $p^{(0)}$ is an initial estimate for p_*, the choice

$$p^{(0)} = \max(0, p_{\mathrm{PVRS}}), \tag{96}$$

where p_{PVRS} is given by (77), provides accurate solutions. In a similar manner, the star state velocity may be calculated from

$$u_* = \frac{1}{2}[u_{\mathrm{L}} + u_{\mathrm{R}} + (p_* - p_{\mathrm{R}})\bar{f}_{\mathrm{R}}(p^{(0)}) - (p_* - p_{\mathrm{L}})\bar{f}_{\mathrm{L}}(p^{(0)})]. \tag{97}$$

The density states ρ_{L}^* and ρ_{R}^* can be calculated from the density–pressure relationships (24) and the tangential velocity is given by Equation (81).

4.3.2. The TSRS using the Tait equation of state. A very similar method exists for the Tait equation of state where

$$\rho_* = \frac{\rho_{\mathrm{L}}\bar{g}_{\mathrm{L}}(\rho^{(0)}) + \rho_{\mathrm{R}}\bar{g}_{\mathrm{R}}(\rho^{(0)}) - \Delta u}{\bar{g}_{\mathrm{L}}(\rho^{(0)}) + \bar{g}_{\mathrm{R}}(\rho^{(0)})}, \tag{98}$$

where

$$\bar{g}_{\mathrm{K}} = \left[\frac{k(\rho_*^n - \rho_{\mathrm{K}}^n)}{\rho_*\rho_{\mathrm{K}}(\rho_* - \rho_{\mathrm{K}})}\right]^{1/2}, \tag{99}$$

and $\rho^{(0)}$ is an initial estimate for ρ_* and

$$\rho^{(0)} = \max(0, \rho_{\mathrm{PVRS}}) \tag{100}$$

is used, where ρ_{PVRS} is given by Equation (87). The solution is completed by calculating

$$u_* = \frac{1}{2}[u_{\mathrm{L}} + u_{\mathrm{R}} + (\rho_* - \rho_{\mathrm{R}})\bar{g}_{\mathrm{R}}(\rho^{(0)}) - (\rho_* - \rho_{\mathrm{L}})\bar{g}_{\mathrm{L}}(\rho^{(0)})], \tag{101}$$

and the tangential velocity is given by Equation (81). Care must be taken with this Riemann solver to avoid division by zero in the trivial case $\mathbf{U}_{\mathrm{L}} = \mathbf{U}_{\mathrm{R}}$. As this Riemann solver first uses the PVRS to calculate p_*, it is easy to detect the case in which it is unnecessary to use this Riemann solver.

4.4. An HLLC Riemann solver

The approximate Riemann solver of Harten, Lax and Van Leer (HLL) has proved very popular within the computational fluid dynamics (CFD) community, and many extensions to it have been made. In the original method, the assumption is made that the solution to the Riemann problem consists of only two waves. One of the extensions to this method is due to Toro *et al.* [17], where the existence of a contact wave or shear wave within the solution was restored. The resulting Riemann solver is called the HLLC Riemann solver.

The HLLC Riemann solution $\mathbf{U}(x, t)$ is given by

$$\mathbf{U}(x, t) = \begin{cases} \mathbf{U}_{\mathrm{L}} & \text{if} \quad x/t \le S_{\mathrm{L}} \\ \mathbf{U}_{\mathrm{L}}^* & \text{if} \quad S_{\mathrm{L}} \le x/t \le S^* \\ \mathbf{U}_{\mathrm{R}}^* & \text{if} \quad S^* \le x/t \le S_{\mathrm{R}} \\ \mathbf{U}_{\mathrm{L}} & \text{if} \quad x/t \ge S_{\mathrm{R}} \end{cases} \tag{102}$$

where S_{L}, S^*, S_{R} are estimates for the three wave speeds, see Figure 3. The solutions for the corresponding fluxes F_{L}^* and F_{R}^* are obtained by rewriting the Euler equations in integral form

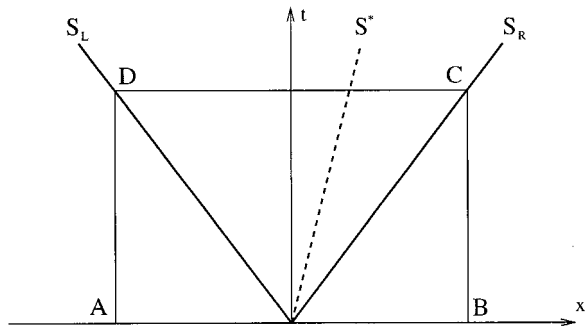

Figure 3. The integration region for the HLLC Riemann solver.

$$\oint (\mathbf{U}\,\mathrm{d}x - \mathbf{F}\,\mathrm{d}t) = 0, \tag{103}$$

and carrying out the integral over the control volume ABCD shown in Figure 3. The result is

$$\mathbf{F}_{\mathrm{L}}^{*} = \mathbf{F}_{\mathrm{L}} + S_{\mathrm{L}}(\mathbf{U}_{\mathrm{L}}^{*} - \mathbf{U}_{\mathrm{L}}), \tag{104}$$

$$\mathbf{F}_{\mathrm{R}}^{*} = \mathbf{F}_{\mathrm{R}} + S_{\mathrm{R}}(\mathbf{U}_{\mathrm{R}}^{*} - \mathbf{U}_{\mathrm{R}}). \tag{105}$$

These two equations can be obtained more directly by applying the Rankine–Hugoniot conditions across each non-linear wave. What remains to be done is to determine $\mathbf{U}_{\mathrm{L}}^{*}$ and $\mathbf{U}_{\mathrm{R}}^{*}$ to be substituted into Equations (104) and (105) to obtain $\mathbf{F}_{\mathrm{L}}^{*}$ and $\mathbf{F}_{\mathrm{R}}^{*}$.

4.4.1. The HLLC Riemann solver using the Tammann equation of state. If the approximation $u^{*} = S^{*}$ is made (104) and (105) can be solved for $\mathbf{U}_{\mathrm{K}}^{*}$ to give

$$\mathbf{U}_{\mathrm{K}}^{*} = \rho_{\mathrm{K}}\left(\frac{S_{\mathrm{K}} - u_{\mathrm{K}}}{S_{\mathrm{K}} - S^{*}}\right)\begin{bmatrix} 1 \\ S^{*} \\ v_{\mathrm{K}} \\ \dfrac{E_{\mathrm{K}}}{\rho_{\mathrm{K}}} + (S^{*} - u_{\mathrm{K}})\left(S^{*} + \dfrac{p_{\mathrm{K}}}{\rho_{\mathrm{K}}(S_{\mathrm{K}} - u_{\mathrm{K}})}\right) \end{bmatrix}. \tag{106}$$

The star state fluxes can then be found by substituting these back into (104) and (105). The HLLC flux may now be computed, which can be written as

$$\mathbf{F}^{\mathrm{HLLC}} = \begin{cases} \mathbf{F}_{\mathrm{L}} & \text{if} \quad x/t \le S_{\mathrm{L}} \\ \mathbf{F}_{\mathrm{L}}^{*} = \mathbf{F}_{\mathrm{L}} + S_{\mathrm{L}}(\mathbf{U}_{\mathrm{L}}^{*} - \mathbf{U}_{\mathrm{L}}) & \text{if} \quad S_{\mathrm{L}} \le x/t \le S^{*} \\ \mathbf{F}_{\mathrm{R}}^{*} = \mathbf{F}_{\mathrm{R}} + S_{\mathrm{R}}(\mathbf{U}_{\mathrm{R}}^{*} - \mathbf{U}_{\mathrm{R}}) & \text{if} \quad S^{*} \le x/t \le S_{\mathrm{R}} \\ \mathbf{F}_{\mathrm{L}} & \text{if} \quad x/t \ge S_{\mathrm{R}}. \end{cases} \tag{107}$$

There are a number of ways in which the wave speeds S_{L}, S^{*} and S_{R} may be calculated. An obvious and straightforward choice would be

$$S_{\mathrm{L}} = u_{\mathrm{L}} - a_{\mathrm{L}}, \qquad S^{*} = u^{*}, \qquad S_{\mathrm{R}} = u_{\mathrm{R}} - a_{\mathrm{R}}. \tag{108}$$

However the preferred method is based on making an initial guess for p^*, in which case discrimination can be made between shocks and rarefactions. If the exact expressions for the wave speeds from Section 2 is taken, the three wave speeds can be written as

$$S_L = u_L - q_L^{(1)} a_L, \qquad S^* = u^*, \qquad S_R = u_R + q_R^{(1)} a_R, \tag{109}$$

where

$$q_K^{(1)} = \begin{cases} 1 & \text{if} \quad p^* \le p_K \\ \left[1 + \dfrac{\gamma+1}{2\gamma} \left(\dfrac{\bar{p}^*}{\bar{p}_K} - 1 \right) \right]^{1/2} & \text{if} \quad p^* > p_K \end{cases}. \tag{110}$$

The choice for p^* can be taken from any of the above approximate Riemann solvers.

4.4.2. The HLLC Riemann solver using the Tait equation of state. Apart from the tangential velocity component, Equations (104) and (105) can then be solved for $\mathbf{U}_L^* = \mathbf{U}_R^*$ to give the (HLL) solution

$$\mathbf{U}^{HLL} = \frac{S_R \mathbf{U}_R - S_L \mathbf{U}_L + \mathbf{F}_L - \mathbf{F}_R}{S_R - S_L}, \tag{111}$$

or the fluxes can be obtained directly from

$$\mathbf{F}^{HLL} = \frac{S_R \mathbf{F}_L - S_L \mathbf{F}_R + S_L S_R (\mathbf{U}_R - \mathbf{U}_L)}{S_R - S_L}. \tag{112}$$

Finally, the tangential momentum flux can be found to be

$$(\rho uv)^{HLL} = \begin{cases} \rho_L u_L v_L & \text{if} \quad x/t \le S_L \\ (\rho u)^{HLL} v_L & \text{if} \quad S_L \le x/t \le S^* \\ (\rho u)^{HLL} v_R & \text{if} \quad S^* \le x/t \le S_R \\ \rho_R u_R v_R & \text{if} \quad x/t \ge S_R \end{cases}, \tag{113}$$

where $(\rho u)^{HLL}$ is taken from (111).

The exact expressions for the wave speeds from Section 2 enable the three wave speeds to be defined

$$S_L = u_L - q_L^{(2)} a_L, \qquad S^* = u^*, \qquad S_R = u_R + q_R^{(2)} a_R, \tag{114}$$

where

$$q_K^{(2)} = \begin{cases} 1 & \text{if} \quad p^* \le p_K \\ \left[1 + \dfrac{(\rho^*/\rho_K)^n - 1}{n(1 - \rho_K/\rho^*)} \right]^{1/2} & \text{if} \quad p^* > p_K \end{cases}. \tag{115}$$

Again, one of the previous Riemann solvers can be used as the preliminary guess for ρ^*.

5. RESULTS

Here three test problems are devised to assess the performance of these proposed Riemann solvers. Since these Riemann solvers were devised for use as part of a Godunov-type numerical scheme, it is the fluxes in the star region that are important to us (aside from in the sonic case). The approximate Riemann solvers will be used to calculate the two star state fluxes $\mathbf{F}_{\mathrm{L}}^{*}$ and $\mathbf{F}_{\mathrm{R}}^{*}$ and then will be compared with the fluxes obtained within the exact solution.

5.1. Test 1

For the Riemann solvers employing the Tammann equation of state the initial conditions in terms of the primitive variables $\mathbf{W} = (\rho, u, v, p)$ were specified. The first test problem has the following initial left and right data states

$$\mathbf{W}_{\mathrm{L}} = \begin{pmatrix} 1100.0 \\ 500.0 \\ 0.0 \\ 5000.0 \end{pmatrix} \quad \text{and} \quad \mathbf{W}_{\mathrm{R}} = \begin{pmatrix} 1000.0 \\ 0.0 \\ 0.0 \\ 0.1 \end{pmatrix}, \tag{116}$$

where the units are kg m^{-3}, m s^{-1} and MPa for density, velocity and pressure, respectively. The constant values for γ and p_{c} are taken to be $\gamma = 7.15$ and $p_{\mathrm{c}} = 300.0$ MPa. The exact solution to this test problem consists of a shock of moderate strength ($M_{\mathrm{s}} = 2.65$) moving to the right, and a leftward travelling rarefaction wave. To compare the accuracy of the approximate Riemann solvers, the difference between the exact fluxes and the approximate fluxes for this Riemann problem are given in Table I. The differences are calculated using

$$\mathbf{F}_{\mathrm{ARS}}^{\mathrm{diff}} = \frac{\mathbf{F}_{\mathrm{ARS}} - \mathbf{F}_{\mathrm{exact}}}{\mathbf{F}_{\mathrm{exact}}}, \tag{117}$$

where $\mathbf{F}_{\mathrm{exact}}$ and $\mathbf{F}_{\mathrm{ARS}}$ are the exact and approximate fluxes, respectively.

Table I. Riemann solver results using the Tammann equation of state

	$\mathbf{F}_{\mathrm{L}}^{*}$			$\mathbf{F}_{\mathrm{R}}^{*}$		
	$(\rho u)_{\mathrm{L}}^{*}$	$(\rho u^2+p)_{\mathrm{L}}^{*}$	$(u(E+p))_{\mathrm{L}}^{*}$	$(\rho u)_{\mathrm{R}}^{*}$	$(\rho u^2+p)_{\mathrm{R}}^{*}$	$(u(E+p))_{\mathrm{R}}^{*}$
$\mathbf{F}_{\mathrm{exact}}$	8.473×10^{5}	3.865×10^{9}	3.582×10^{12}	1.035×10^{6}	4.019×10^{9}	3.645×10^{12}
$\mathbf{F}_{\mathrm{PVRS}}^{\mathrm{diff}}$	4.606×10^{-2}	1.019×10^{-1}	1.980×10^{-1}	9.245×10^{-2}	1.145×10^{-1}	2.044×10^{-1}
$\mathbf{F}_{\mathrm{TSRS}}^{\mathrm{diff}}$	-1.761×10^{-2}	7.295×10^{-3}	-9.294×10^{-3}	-1.990×10^{-2}	5.126×10^{-3}	-1.034×10^{-2}
$\mathbf{F}_{\mathrm{TRRS}}^{\mathrm{diff}}$	3.904×10^{-2}	-3.420×10^{-2}	9.768×10^{-4}	1.553×10^{-1}	-3.881×10^{-3}	1.547×10^{-2}
$\mathbf{F}_{\mathrm{HLLC}}^{\mathrm{diff}}$	-1.145×10^{-2}	-3.497×10^{-2}	-3.838×10^{-2}	-2.763×10^{-2}	-2.050×10^{-2}	-3.931×10^{-2}

The first line of results gives the actual flux values obtained using the exact Riemann solver and the following lines give the difference between these values and the values obtained using the approximate Riemann solvers, $\mathbf{F}_{\mathrm{ARS}}^{\mathrm{diff}}$, see Equation (117).

Table II. Riemann solver results using the Tait equation of state

	F*	
	$(\rho u)^*$	$(\rho u^2+p)^*$
$\mathbf{F}_{\text{exact}}$	2.026×10^{5}	3.813×10^{3}
$\mathbf{F}^{\text{diff}}_{\text{PVRS}}$	1.392×10^{-4}	1.170×10^{-2}
$\mathbf{F}^{\text{diff}}_{\text{TSRS}}$	5.266×10^{-4}	-6.411×10^{-4}
$\mathbf{F}^{\text{diff}}_{\text{TRRS}}$	-3.367×10^{-3}	3.327×10^{-3}
$\mathbf{F}^{\text{diff}}_{\text{HLLC}}$	9.904×10^{-4}	1.160×10^{-3}

The first line of results gives the actual flux values obtained using the exact Riemann solver and the following lines give the difference between these values and the values obtained using the approximate Riemann solvers, $\mathbf{F}^{\text{diff}}_{\text{ARS}}$, see Equation (117).

Although these results give an insight into the accuracy, one may expect from these Riemann solvers that it is not possible to put them into a strict-order based on their accuracy. However, the following observations may be made: The PVRS Riemann solver is consistently the least accurate of the four as expected; it is however, the cheapest Riemann solver in terms of CPU time, as it makes fewer calculations. At the other end of the scale, the TSRS Riemann solver appears to be the most accurate Riemann solver for this test problem. The HLLC and TRRS Riemann solvers provide slightly less accurate results than the TSRS, but both are significantly more accurate than the PVRS.

5.2. Test 2

For the Tait equation of state, the initial left and right data states in terms of the primitive variable $\mathbf{W}=(\rho, u, v)$ are described,

$$\mathbf{W}_{\text{L}}=\begin{pmatrix}1100.0\\200.0\\0.0\end{pmatrix}\quad\text{and}\quad\mathbf{W}_{\text{R}}=\begin{pmatrix}1000.0\\0.0\\0.0\end{pmatrix}. \tag{118}$$

The constant values $\rho_0=997.04\ \text{kg m}^{-3}$, $n=7.15$ and $B=300$ Mpa are assumed. The exact solution to this test problem consists of a weak shock ($M_{\text{s}}=1.25$) moving to the right and a rarefaction wave moving to the left. The results of solving this Riemann problem with the Riemann solvers employing the Tait equation of state are shown in Table II, again the performance of the approximate Riemann solvers are compared by looking at the difference between the approximate fluxes and the exact flux computed using Equation (117). One can see from these results that again, the TSRS appears to be the most accurate of the approximate Riemann solvers. The PVRS Riemann solver does better in this test as the shock wave is weaker. It must be noted that none of these Riemann solvers performs badly.

5.3. Implementation of Riemann solvers into Godunov-type methods

Here an example of how the present Tammann equation of state Riemann solvers can perform in a numerical scheme is given. For simplicity of comparison, the first-order accurate Godunov scheme [18] is used. In this method, the solution vector, **U**, is taken to be piecewise constant throughout the domain and the solution value in each cell is representative of an integral average. The solution is advanced by solving the set of Riemann problems between

neighbouring constant states $(\mathbf{U}_i^n, \mathbf{U}_{i+1}^n)$. The local solution taken along the ray $x/t = 0$, denoted by $\mathbf{U}^*_{i+1/2}(0)$, is used to calculate the intercell fluxes and it is updated to the next time level using the conservative formula

$$\mathbf{U}_i^{n+1} = \mathbf{U}_i^n - \frac{\Delta t}{\Delta x}\left[\mathbf{F}(\mathbf{U}^*_{i+1/2}(0)) - \mathbf{F}(\mathbf{U}^*_{i-1/2}(0))\right]. \tag{119}$$

The time step is calculated based on the characteristic speeds in the solution such that the CFL condition $C = \Delta t/\Delta x\, S_{\max} < 1$ is satisfied, where $S_{\max}$ is the maximum characteristic speed and $C = 0.9$ is taken. Consider a shock tube of unit length with a diaphragm at $x = 0.5$ separating two liquid states given by Equation (116). At $t = 0.0$, the diaphragm is instantaneously removed, and the resulting flow consists of a shock wave, a contact wave and a rarefaction wave.

Figure 4 shows the results of applying the Godunov method to this problem employing the exact Riemann solver throughout the domain. The number of computational cells, N, is taken to be 100 such that the cell size $\Delta x = 1/100$. The results obtained using the approximate Riemann solvers in place of the exact Riemann solver are so similar to the results of Figure 4 that it serves no purpose to show them all here, therefore just a plot the results using the HLLC Riemann solver as an example, will be given, see Figure 5. Of course in practice, higher-order accuracy is needed. The weighted average flux (WAF) method of Toro [19] is a second-order accurate extension of Godunov's method. In this method, the intercell fluxes are

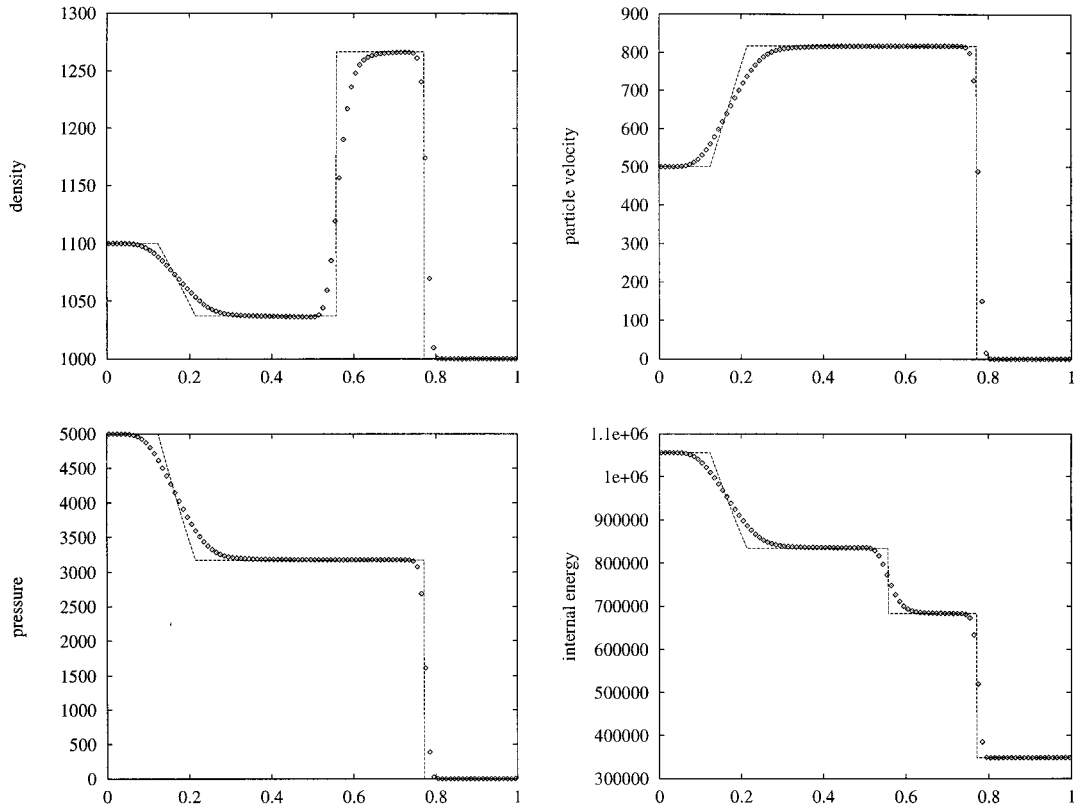

Figure 4. Dotted line—exact solution, symbols—Godunov's method using the exact Riemann solver.

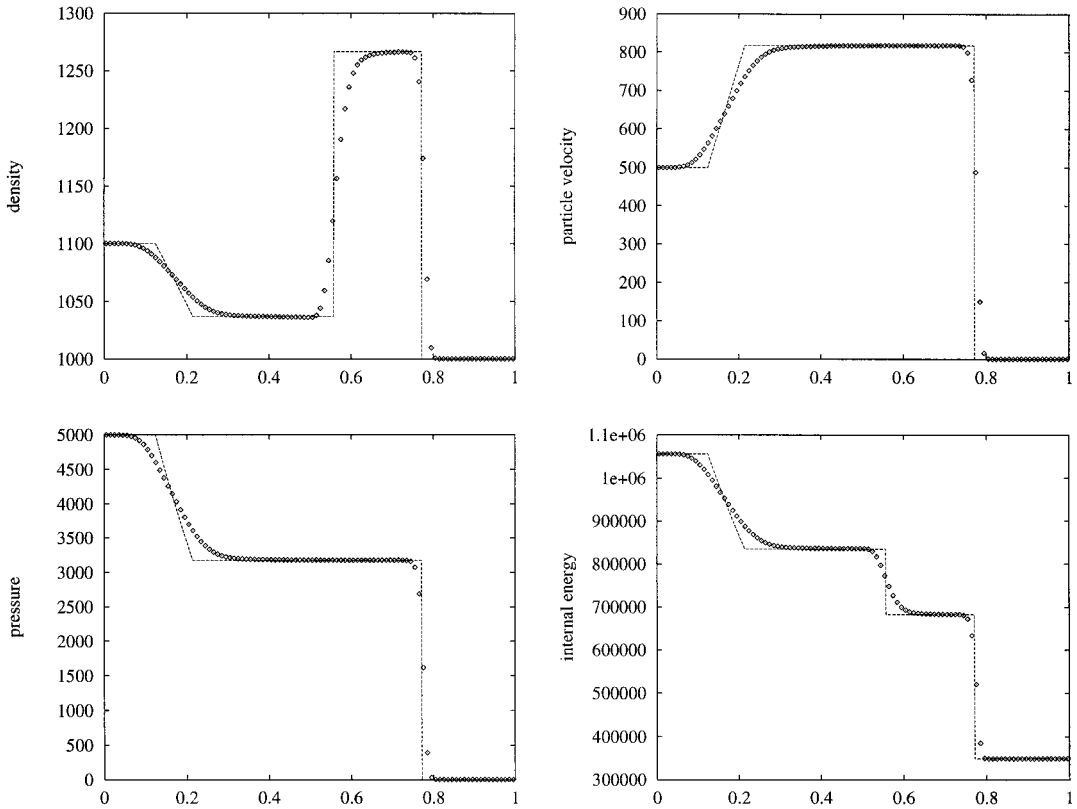

Figure 5. Dotted line—exact solution, symbols—Godunov's method using the HLLC Riemann solver.

calculated by approximating an integral average of the fluxes within the solution of the Riemann problem. Figure 6 shows the results of applying the WAF method, also with $N = 100$, to this test problem utilising the PVRS Riemann solver. Both these first- and second-order methods converge to the correct solution as the mesh is refined, although the first-order method's convergence rate is considerably slower.

If the numerical solution obtained by using Godunov's method is denoted with an exact, PVRS, TSRS, TRRS, HLLC Riemann solver as $\mathbf{U}^{\text{exact}}$, $\mathbf{U}^{\text{PVRS}}$, $\mathbf{U}^{\text{TSRS}}$, $\mathbf{U}^{\text{TRRS}}$ and $\mathbf{U}^{\text{HLLC}}$, respectively, a comparison between the approximate Riemann solver solutions and the exact Riemann solver solution can be made by comparing the total energy at each grid point. If the calculations below are made,

$$err = \frac{1}{N} \sum_{i=1}^{N} \frac{|E_i^{\text{exact}} - E_i^{\text{ARS}}|}{E_i^{\text{exact}}}, \tag{120}$$

where ARS is PVRS, TSRS, TRRS or HLLC, and take the number of grid points to be $N = 100$, the results displayed in Table III are obtained. Here it can be seen that, consistent with the results of Test 1, the Riemann solver TSRS is the most accurate, followed fairly closely by the TRRS and HLLC Riemann solvers. The PVRS Riemann solver is the least accurate of the four Riemann solvers. However, this is not always the case. If the strength of the shock in this test problem is reduced by reducing the pressure in the left state by a factor

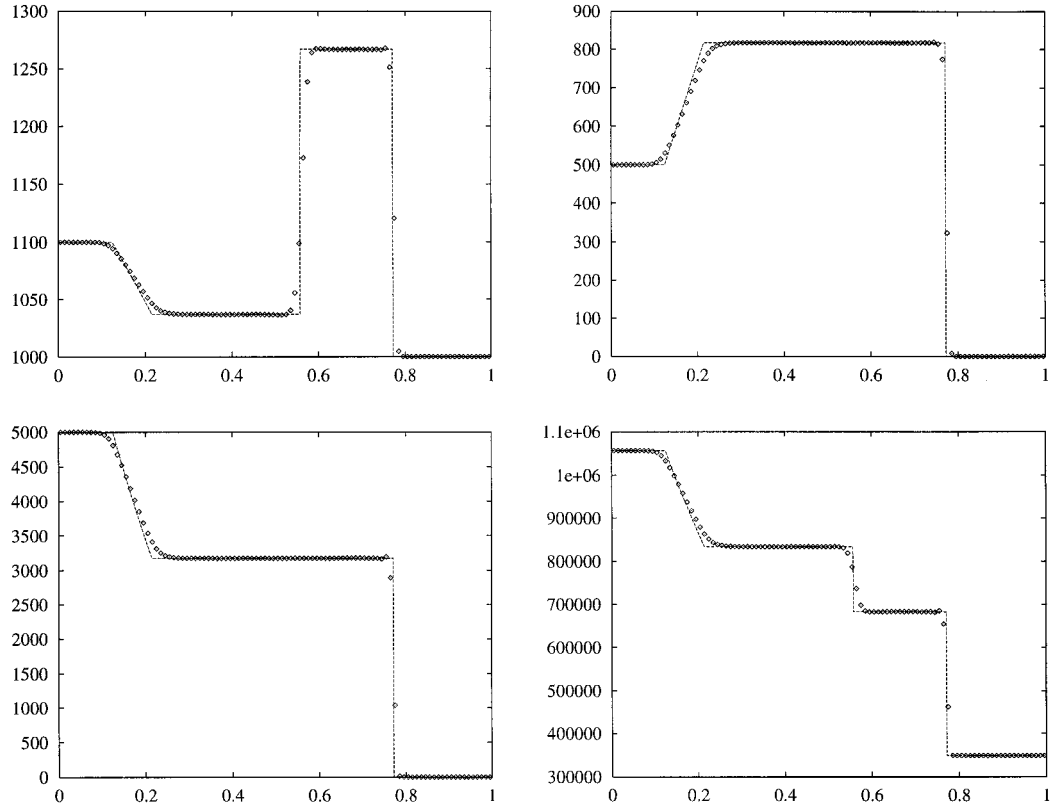

Figure 6. Dotted line—exact solution, symbols—the WAF method using the primitive variable Riemann solver.

of 100 to $p_L = 50$ Mpa, a test problem is obtained in which the shock Mach number $M_s = 1.44$. If the calculations using (120) are made, the results are quite different, see Table IV. In this case, the HLLC Riemann solver is the most accurate followed by the TRRS and the TSRS. The PVRS Riemann solver is again the least accurate. Weak shocks are not the only case in which the HLLC Riemann solver performs the best.

Table III. A comparison between the total energy obtained using the approximate Riemann solvers with the exact Riemann solver

	$err \times 10^{-6}$
PVRS	225.8
TSRS	11.41
TRRS	38.22
HLLC	80.53

Table IV. Results of making the calculations (120) applied to the weakened shock version of Test 1

	$err \times 10^{-6}$
PVRS	116.3
TSRS	21.13
TRRS	16.66
HLLC	5.86

5.4. A sonic test problem

For this test problem, the initial values for $\mathbf{W} = (\rho, u, v, p)$ are taken to be

$$\mathbf{W}_L = \begin{pmatrix} 1000.0 \\ 2000.0 \\ 0.0 \\ 500.0 \end{pmatrix} \quad \text{and} \quad \mathbf{W}_R = \begin{pmatrix} 1000.0 \\ 2000.0 \\ 0.0 \\ 1.0 \end{pmatrix}. \tag{121}$$

Although this test problem is artificial, as are many other classical test problems of this nature, it is useful for highlighting an area in which the performance of the Riemann solvers differ greatly. The exact solution to this test problem consists of a right-going shock wave with $M_s = 2.6$, and a sonic rarefaction wave. Figure 7 shows the results of applying the Godunov method with exact, HLLC and TSRS Riemann solvers, respectively. Note that plotting the results for the TRRS and PVRS Riemann solvers has been omitted as these perform in a very similar manner to those of the TSRS Riemann solver. The results show that the HLLC Riemann solver is the only one that is able to provide a smooth solution through the sonic rarefaction wave; in fact even the exact Riemann solver solution is not smooth around the sonic point, although the scheme is entropy satisfying [20].

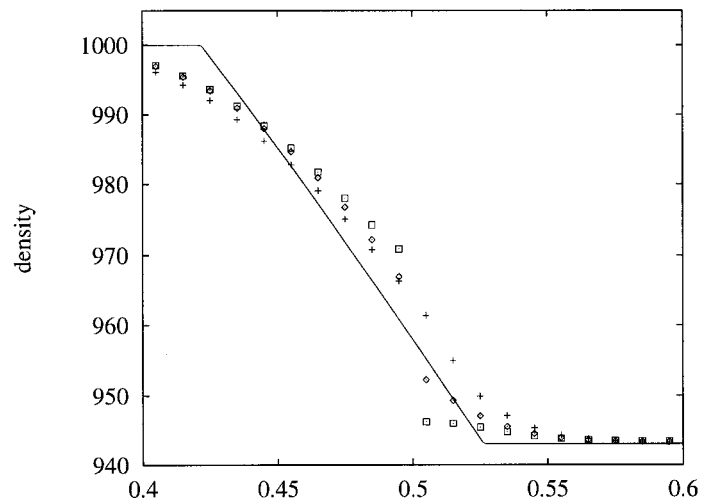

Figure 7. Solid line—exact solution, symbols—Godunov's method using the following Riemann solvers: crosses, HLLC; squares, TSRS; diamonds, exact. The initial discontinuity lies at $x_0 = 0.5$.

6. CONCLUSIONS

It has been shown that a number of Riemann solvers, originally formulated for the solution of gas dynamical problems, can be easily adapted for hydrodynamic problems. Full descriptions of two exact Riemann solvers has been given for liquids corresponding to two choices of equation of state, namely the Tammann and Tait equations of state. These exact Riemann solvers involve finding the solution to a single non-linear algebraic equation for one of the star state variables, and both Riemann solvers converge quickly to the correct solution. These Riemann solvers have all been designed for use as part of a numerical scheme in mind. It is clear that for complex flows in multidimensions, the use of an exact Riemann solver would be too time consuming and that the use of approximate Riemann solvers will become necessary. The proposed approximate Riemann solvers should prove satisfactory for this task. It was found that the HLLC Riemann solver is the most accurate Riemann solver for flows that do not contain strong shock waves. This is especially true where the flow contains sonic rarefaction waves. The PVRS, TSRS and TRRS Riemann solvers perform badly in this case. For flows containing strong shocks, the TSRS Riemann solver is the most accurate. The PVRS Riemann solver is the least accurate Riemann solver here, although its cheapness can prove very useful in situations where only a limited amount of information is needed about the solution to the Riemann problem. It is apparent that no one approximate Riemann solver performs consistently better than any of the others under all flow conditions. It is therefore an obvious progression to use the approximate Riemann solvers adaptively. For example, it has been shown that the PVRS works particularly well when used adaptively with the exact Riemann solver [15].

Currently, work on modelling complex flow problems that involve both gas and water media is in progress. It is expected that the Tammann equation of state will prove to be very useful for this application.

REFERENCES

1. P.A. Thompson, *Compressible Fluid Dynamics*, McGraw-Hill, New York, 1972.
2. H.-T. Chen and R. Collins, 'Shock wave propagation past an ocean surface', *J. Comp. Phys.*, **7**, 89–101 (1971).
3. B. Koren, P.F.M. Michielsen, J.W. Kars and P. Wesseling, 'A computational method for high-frequency oleodynamics, application to hydraulic shock-absorber designs', in *The Third ECCOMAS Computational Fluid Dynamics Conference*, Wiley, New York, 1996, pp. 7225–731.
4. J. Flores and M Holt, 'Glimms method applied to underwater explosions', *J. Comp. Phys.*, **44**, 377–387 (1981).
5. J.G. Kirkwood and H. Bethel, 'The pressure wave produced by an underwater explosion', *OSRD Rep. 588* and *813*, part I and III, Department of Commerce bibliography *PB 32184*, 1942.
6. P.G. Tait, *Collected Scientific Papers*, vol. 2, Cambridge University Press, Cambridge, 1900.
7. J.O. Hirschtelder, C. Curtiss and R. Bird, *Molecular Theory of Gases and Liquids*, Wiley, New York, 1964.
8. T. Sugimura, K. Tokita and T. Fujiwara, 'Non-steady shock wave propagating in a bubble–liquid system', *Rep. Fac. Sci. Tech. Meijo University* (Japan), **24**, 67–76 (1984).
9. M.J. Ivings, D.M. Causon and E.F. Toro, 'Riemann solvers for compressible water', in *The Third ECCOMAS Computational Fluid Dynamics Conference*, Wiley, New York, 1996, pp. 944–949.
10. J.E. Jackson Jr. and M.A. Jamnia, 'Non-linear FSI due to underwater explosions', *J. Eng. Mech.*, **110**, 507–517 (1984).
11. C.H. Cooke and T. Chen, 'On shock capturing for pure water with general equation of state', *Comm. Appl. Numer. Methods*, **8**, 219–233 (1992).
12. F. Lennon, '*Shock Wave Propagation in Water*', PhD thesis, Department of Mathematics and Physics, Manchester Metropolitan University, 1994.
13. W.F. Ballhaus and M. Holt, 'Interaction between the ocean surface and underwater spherical blast waves', *Phys. Fluid*, **17**, 1068–1079 (1974).
14. E.F. Toro, *Riemann Solvers and Numerical Methods for Fluid Dynamics*', Springer, Berlin, 1997, to appear.
15. E.F. Toro, 'A linearised Riemann solver for the time-dependent Euler equations of gas dynamics', *Proc. R. Soc. Lond. A*, **434**, 683–693 (1991).

16. E.F. Toro, 'Direct Riemann solvers for the time-dependent Euler equations', *Shock Waves*, **5**, 75–80 (1995).
17. E.F. Toro, M. Spruce and W Speares, 'Restoration of the contact surface in the HLL Riemann solver', *Shock Waves*, **4**, 25–34 (1994).
18. S.K. Godunov, 'A difference method for the numerical calculation of discontinous solutions of hydrodynamic equations', *Mat. Sb.*, **47**, 271–306 (1959).
19. E.F. Toro, 'The weighted average flux method applied to the Euler equations', *Philos. Trans. R. Soc. Lond. A*, **341**, 325–339 (1992).
20. A. Harten, P.D. Lax and B. van Leer, 'On upstream differencing and Godunov-type schemes for hyperbolic conservation laws', *SIAM Rev.*, **25**, 35–61 (1983).

